PCCP

ROYAL SOCIETY OF CHEMISTRY

PAPER

View Article Online
View Journal

Cite this: DOI: 10.1039/d3cp01136d

The high-accuracy spectroscopy of H_2 rovibrational transitions in the (2-0) band near 1.2 μm

H. Fleurbaey, [a] A. O. Koroleva, [ab] S. Kassi [a] and A. Campargue *[a]

Accurate transition frequencies of six lines of the (2-0) vibrational band of H_2 are reported near 1.2 μm, namely Q1–Q4, S0, and S1. These weak electric-quadrupole transitions were measured at room temperature by comb-referenced cavity ring-down spectroscopy. Accurate transition frequencies were determined by applying a multi-spectrum fit procedure with various profile models including speed-dependent collisional broadening and shifting phenomena. Although none of the considered profiles allows reproducing the shape of the strongest lines at the noise level, the zero-pressure line centers are found mostly independent of the used profile. The obtained values are the first H_2 (2-0) transition frequencies referenced to an absolute frequency standard. As a result, a 1σ-accuracy better than 100 kHz was achieved for the Q1, S0, and S1 transition frequencies, improving by three orders of magnitude the accuracy of previous measurements. For the six measured transitions, the most recent calculated frequencies were found to be systematically underestimated by about 2.51 MHz, about twice their claimed uncertainties. The energy separation between J = 2 and J = 0 rotational levels of the vibrational ground state was derived from Q2 and S0 transition frequencies and found within the 110 kHz uncertainty of its theoretical value. The same level of agreement was achieved for the energy separation between the J = 3 and J = 1 rotational levels obtained by the difference of Q3 and S1 transition frequencies. The *ab initio* values of the intensity of the six transitions were validated within a few thousandths.

Received 13th March 2023,
Accepted 29th April 2023

DOI: 10.1039/d3cp01136d

rsc.li/pccp

Introduction

Due to its simplicity, dihydrogen (H_2) and its isotopologues (HD and D_2) are quantum physics test systems for advanced theoretical calculations including nonadiabatic, relativistic, quantum electrodynamics (QED) effects[1–3] and hyperfine structure calculations.[4–6] For instance, the measurement of highly accurate rotation–vibration (RV) transition frequencies provides stringent tests of the level energies recently obtained by fully variational calculations including high-level QED corrections.[1–3] In recent years, significant progress has resulted from the fruitful emulation between theory and experiment. Due to the weakness of the considered RV transitions, precision spectroscopy is experimentally challenging in H_2. As a homonuclear diatomic molecule, H_2 has no electric dipole spectrum, and its RV spectrum is formed by very weak electric-quadrupole vibrational bands, (V-0), of decreasing intensity (see Fig. 6 of ref. 7). For instance, the (1-0) fundamental and (2-0) first overtone bands centered at about 4160 and 8090 cm^{-1}, have maximum line intensities of 3.2×10^{-26} and 5.2×10^{-27} cm per molecule at 296 K, respectively. In recent years, hydrogen deuteride (HD) has been preferred for metrological measurements because HD shows stronger absorption bands than H_2. This is due to the charge asymmetry, resulting in a weak dipole moment existing in this heteronuclear isotopologue thus giving rise to a small electric dipole moment. As a result, in the (2-0) band, the electric dipole transitions in HD are about two orders of magnitude stronger than electric quadrupole transitions in H_2 (and HD).

Accuracies better than 100 kHz level have been recently achieved by several groups for a few (2-0) transition frequencies in HD.[8–17] This level of accuracy represents about one-thousandth of the Doppler width of the (2-0) HD transitions at room temperature. Part of the experimental studies was performed in saturation regime in order to circumvent this large Doppler broadening but underlying hyperfine components were found to lead to a dispersive-like spectral structure which limited the final accuracy on the line center determination.[8,10–12,14] As a result, accuracies on HD transition frequencies achieved in the saturation regime are similar to those obtained in the Doppler regime[15,16] in particular at low temperatures.[17]

To the best of our knowledge, in the case of the H_2 major isotopologue, no RV transition frequencies have been reported

[a] Univ. Grenoble Alpes, CNRS, LIPhy, Grenoble, France.
E-mail: alain.campargue@univ-grenoble-alpes.fr
[b] Institute of Applied Physics of RAS, Nizhniy Novgorod, Russia

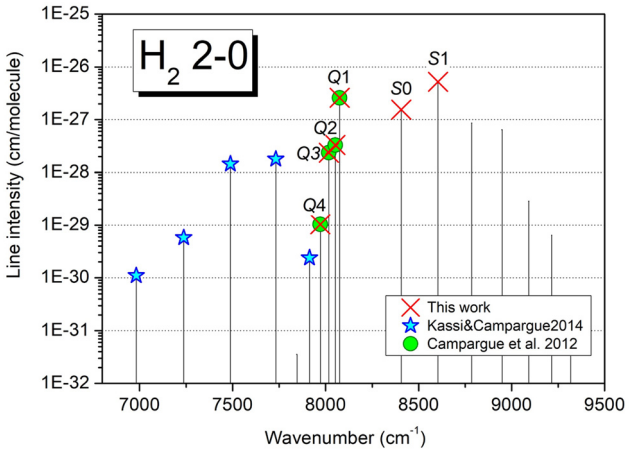

Fig. 1 The calculated stick spectrum of the (2-0) band of H_2.[21] Absorption lines previously measured by CRDS[7,20] are highlighted. Rotational labeling is indicated for the six transitions presently measured.

with sub-MHz accuracy, so far. This situation results both from the above-mentioned weakness of the H_2 RV transitions and from the lack of recent measurements of H_2 spectra referenced to frequency standards. In this context, let us mention the S3 electric-quadrupole transition of the (3-0) band near 795 nm reported with a 1.6 MHz accuracy by measuring the frequency shift to an Rb line.[18,19] Regarding the (2-0) band presented in Fig. 1, the most accurate measurements were performed in our group using high-sensitivity cavity ring-down spectroscopy (CRDS), but the frequency calibration of these spectra was based on nearby reference lines of water vapor (present as an impurity in the H_2 cell).[7,20] As a result, the claimed uncertainty on the reported transition frequencies was no better than 10^{-3} cm^{-1} (30 MHz).

In the present work, we report a gain of up to three orders of magnitude on high-accuracy frequency measurements of the Q1–Q4 transitions and complement the dataset with S0 and S1, in the (2-0) vibrational band of H_2. The measurements were performed in the Doppler regime at room temperature, by comb-referenced cavity ring-down spectroscopy. As mentioned above, the Q1–Q4 transitions have been measured in ref. 20 using standard CRDS, while the S0 and S1 transitions were apparently not revisited since the recordings of Bragg *et al.* in 1982.[22] These authors used a Kitt Peak Solar Fourier transform spectrometer with an absorption path length of 434 m and pressure values of 1.4 and 2.8 atm.

Let us recall that the determination of the transition frequencies in the Doppler regime requires correcting the pressure-induced line shift in order to extrapolate the line center at zero pressure limit. This necessitates a careful line profile analysis of a series of recordings at different pressures to determine the pressure dependence of each spectroscopic parameter. As non-Voigt line-shape effects (*e.g.* Dicke narrowing and speed-dependent effects) are exceptionally pronounced in the case of H_2 (see ref. 23 and ref. 24), sophisticated line shapes such as the speed-dependent Nelkin–Ghatak profile will be used in the forthcoming analysis. Note that the high sensitivity provided by cavity-enhanced techniques such as CRDS is a crucial advantage for high-quality recordings at low pressure (*e.g.* a few Torr in the present case of the Q1, S0, and S1 lines), which limits the uncertainty on the line center extrapolation at zero-pressure.

The experimental setup and the recording procedure are described in the following section. In the next one, we present the frequency determination of the different transitions from a multi-spectrum fit of the series of spectra recorded at different pressures. The obtained transition frequencies are compared with the theory in the penultimate section, before the concluding remarks.

Experiment

The room temperature absorption spectrum of natural dihydrogen (Alphagaz2, 99.9999% chemical purity) was recorded in the flow regime using high sensitivity frequency comb referenced cavity ring-down spectroscopy. The frequency comb referenced CRDS (CR-CRDS) method and setup used for the recordings have been described in detail in ref. 25 and 26. The accurate frequency values associated "on the fly" to each ring-down event allow not only an absolute calibration of the frequency axis but also a reduction of the noise amplitude, in particular on the sharp slopes of the line profiles.[27,28]

The recording procedure is similar to that adopted to measure D_2 transitions in the (2-0) band[26,29,30] except that an external cavity diode laser (ECDL) is used as a light source instead of distributed-feedback (DFB) laser diodes. The ECDL (Toptica fiber-connected DL pro, 1200 nm) was tuned to record small spectral intervals around the Q1–Q4, S0, and S1 transitions spanning the 7970–8605 cm^{-1} region. For the evacuated cavity, the ring-down time τ_0 varied from about 180 μs to 360 μs depending on the wavenumber. For each frequency point, about 50 to 120 ring-downs were averaged leading to a minimum detectable absorption coefficient between 2×10^{-12} and 6×10^{-11} cm^{-1} for a single scan. Following ref. 27 and 29, a self-referenced frequency comb (Model FC 1500-250 WG from Menlo Systems) was used for the frequency calibration of the spectra. The frequency attached to each ring-down event is determined from (i) the frequency measurement of the beat note between a fraction of the ECDL light and a tooth of the frequency comb and (ii) the tooth number deduced from the frequency value provided by a commercial Fizeau-type wavemeter (HighFinesse WSU7-IR, 5 MHz resolution, 20 MHz accuracy over 10 hours). For each frequency step, the average central emission frequency of the ECDL was actively stabilized using a software-based Proportional-Integral loop, with a 100 Hz bandpass, acting on the laser current.

A drawback of Doppler-limited absorption spectroscopy compared to Doppler-free saturation spectroscopy is that the retrieved line parameters can be affected by interferences with lines due to gas impurities present in the cell. Water vapor desorbing from the CRDS cell or from the injection tubes is the most problematic species. In order to minimize the concentration of gas impurities, the spectra were recorded in the flow regime. As explained in the next section, water lines were

Table 1 Summary of the recordings of the Q1–Q4, S0 and S1 (2-0) transitions of H_2

	Q4	Q3	Q2	Q1	S0	S1
Position[21] (cm^{-1})	7971.1001	8017.1831	8051.9877	8075.3074	8406.3609	8604.2151
Intensity[21] (cm per molecule)	1.04×10^{-29}	2.36×10^{-28}	3.29×10^{-28}	2.60×10^{-27}	1.56×10^{-27}	5.24×10^{-27}
Pressure (Torr)	Number of recordings					
1				[a]	63	31
5				[a]	50	40
10		34	63	10 [a]	19	11
45		5	7	8	51	40
90	5	6	5	10	16	
210	6	5	7	10	57	
500	7	6	6	8	72	
750	7	7	5	6	36	

[a] Additional series of 30 to 100 spectra were recorded for pressures between 2 and 10 Torr, with a pressure step of 1 Torr. These spectra (525 in total) were analyzed as an independent dataset.

apparent in some of the spectra and allowed us to estimate the water concentration in the cell to be typically a few tens of ppm.

The hydrogen pressure in the CRDS cell was actively regulated to values between 1.0 and 750 Torr through a needle valve connecting the cell to a turbo pump group, using a computer-based Proportional/Integral controller. The gas pressure in the cell was continuously monitored by two capacitance gauges (MKS Baratron, 10 Torr, and 1000 mbar full range). For each line, the recordings were performed for a series of pressure values listed in Table 1. The range of the pressure values depends on the line intensities. In the case of the Q4 line, which has the smallest intensity (about 10^{-29} cm per molecule), a minimum pressure value of 90 Torr was used as the quality of the spectra was insufficient at lower pressure. In the case of the strongest lines (Q1, S0, and S1) which have an intensity larger than 10^{-27} cm per molecule range, recordings could be performed down to 1 Torr. The strong pressure impact on the line profiles is illustrated in Fig. 2. For each line, the absorption coefficients obtained for the lowest and highest pressure values were divided by the pressure values (in Torr) and superimposed. The self-induced pressure shift of the line centre and the narrowing of the profile at higher pressure are clearly observed. From the relative area of water lines visible in S0 and S1 spectra one concludes that water is essentially desorbed from the tubing and/or cell rather than present in the sample bottle, as its relative amount clearly varies with pressure.

In order to improve the line parameter determinations, for each pressure value, a number of spectra were recorded successively (from 5 to 72 – see Table 1). The duration of a single scan was about 20 minutes. Special efforts were made to accumulate spectra for the lowest pressure values, which are crucial to minimizing the uncertainty on the zero-pressure line position. In the case of the Q1 line, in addition to the recordings listed in Table 1, a series of 30 to 100 spectra were recorded between 2 and 10 Torr, with a pressure step of 1 Torr (525 spectra in total). These spectra were analyzed as an independent dataset because that measurement campaign was separated from the others by several years. The temperature varied between 294.0 and 295.4 K according to the recordings.

We recall that the studied H_2 lines were observed superimposed on the broad H_2 collision-induced absorption (CIA) band which extended from 7800 to 9200 cm^{-1}.[31,32] In the present recordings, limited to narrow spectral intervals around the H_2 lines, the CIA shows up as an increase in the baseline level of the CRDS spectra. Due to the dipole moments induced by interactions between colliding H_2 molecules, the CIA has a pressure-squared dependence. The sensitivity of the CRDS technique and the stability of the setup allows for the measurements of such weak CIA at sub-atmospheric pressures. In ref. 20, the P^2 dependence of the baseline level around the Q1 line was checked up to 1 atm and the corresponding CIA binary cross-section coefficient was determined. Systematic measurements of the H_2 CIA first overtone band in the region accessible with the current ECDL (8000–8650 cm^{-1}) will be undertaken in the future for validation tests of the semi-empirical CIA values[31,32] largely used for planetary applications.

Line parameter retrieval

As mentioned earlier, the standard Voigt profile is not sufficient to adequately model the data due to the prevalence of narrowing effects in H_2, justifying the use of more sophisticated line shapes. The Nelkin–Ghatak profile (NGP) includes the Dicke effect, characterized by the frequency of the velocity-changing collision parameter, ν_{VC}, in the hard-collision model. The quadratic speed-dependent Nelkin–Ghatak profile (qSDNGP) further takes into account the speed dependence of the broadening and shift (γ_2 and δ_2, respectively), modeled with a quadratic law, leading to a narrowing and asymmetry of the line profile. As for the self-induced pressure shift and broadening (δ_0, and γ_0, respectively), the unit of the ν_{VC}, γ_2, and δ_2 parameters is cm^{-1} atm^{-1}. The fitting program MATS[33] developed at NIST, based on the HAPI Python library and the Levenberg–Marquardt minimizing algorithm, was used to fit the parameters of the qSDNG profile to the spectra.

The recorded spectra were typically 0.5 cm^{-1} wide. Some of the lines (S1, S0, and Q1) were affected by the interference from strong water lines in the same spectral region present due to outgassing (see Fig. 2). These water lines were identified on the basis of a recently published[34] line list. In the case of the S1 line, an $H_2{}^{17}O$ line was situated less than 0.05 cm^{-1} from the H_2 line, strongly affecting the observed position if it was not

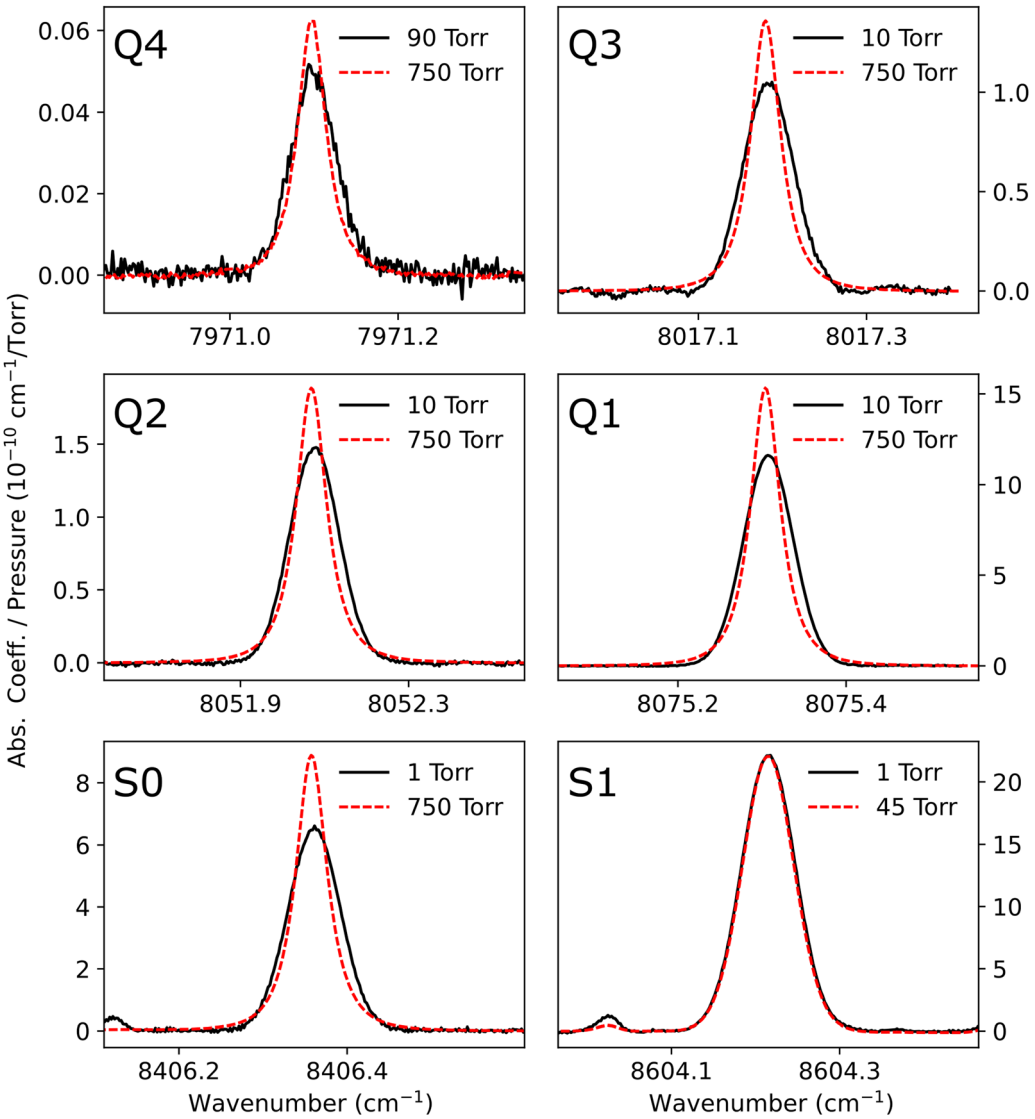

Fig. 2 Comparison of the profiles of the six (2-0) H_2 lines observed in this work, for the lowest and highest pressure value of each dataset. For the clarity of the figure, the absorption coefficients have been corrected from the baseline and divided by the pressure values in Torr. Note the pressure shift of the line centre and the narrowing of the profile at higher pressure.

included in the fit. The observed isotopic abundance of $H_2{}^{17}O$ and HDO was very different from the natural abundance due to previous measurements of isotopically enriched water in the same CRDS cell and were determined experimentally by recording spectra while evacuating the cell. In the analysis, water lines were simulated as Voigt profiles using line parameters from ref. 34. The water mole fraction was floated during the analysis of the S1, S0, and Q1 spectra, and varied between approximately 10 and 200 ppm, well beyond the sub-ppm amount stated in the gas sample. No water interference was observed for the other Q lines.

The analysis was performed in two steps, separately for each line. Firstly, a subset of spectra (one for each pressure value) was fit in a multi-spectrum configuration to determine the line shape parameters (broadening, speed-dependent parameters for more advanced profiles). The multi-spectrum fitting procedure constrained the pressure broadening coefficient (γ_0) and the ν_{VC}, γ_2, δ_2 parameters to be identical for the different pressure values, but the positions and line areas were fitted independently for each spectrum, δ_0 being fixed to zero. The baseline of each spectrum was adjusted as a linear function of frequency. Fig. 3 presents such a subset of spectra for the Q1 and Q2 lines, along with the (meas.-calc.) residuals from the multi-spectrum fits (panel (b)). Note the increase of the baseline level with increasing pressure due to the CIA. The line shape parameters (γ_0, ν_{VC}, γ_2, δ_2) obtained for each transition are given in Table 2. We have also tried fitting the line shape parameters separately for each pressure value, fitting all spectra recorded at a given pressure value together. As can be seen in the lower panel (c) of Fig. 3, the fit quality is better. Nevertheless, the line parameters appear to vary in a somewhat non-linear manner with pressure and the speed-dependent shift parameter δ_2 could not be determined with good precision at lower pressure values

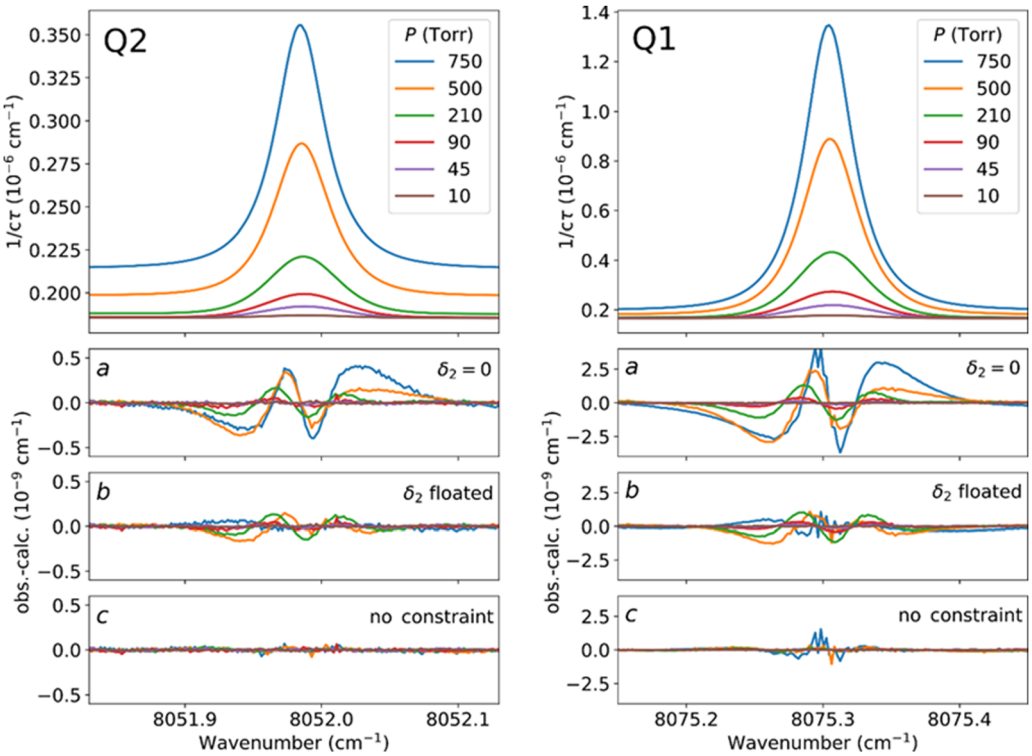

Fig. 3 Sample of spectra of the Q2 (left) and Q1 (right) lines, recorded at various pressures and used to determine the line shape parameters. The panels present the experimental spectra (top), and the residuals of a multi-spectrum fit with qSDNGP profile and three different configurations: with all parameters constrained and δ_2 fixed to zero (a), or δ_2 floated (b); with all parameters determined separately for each pressure (c). Note the different vertical scales for the two lines, and the increase in the baseline at higher pressure due to the CIA.

Table 2 Line shape parameters obtained from multi-spectrum treatment of the CRDS spectra recorded for a series of pressure values using a qSDNGP profile. δ_0, γ_0, ν_{VC}, γ_2, and δ_2 values are given in 10^{-3} cm^{-1} atm^{-1} unit. For a pressure series, the γ_0, ν_{VC}, γ_2, and δ_2 values were constrained to be identical but the line centers and line areas were fitted independently for each spectrum and used afterwards to derive the zero-pressure position (ν_0), line intensity (S) and self-pressure shift (δ_0). The line intensity was directly converted to the reference temperature 296 K in the MATS program. For each line, the line position and shift obtained using the simpler NGP profile (with no speed dependence, *i.e.*, γ_2 and δ_2 fixed to zero) are given in the row below. The uncertainties given within parenthesis in the unit of the last quoted digit correspond to the (1σ) statistical values provided by the fit

	ν_0 (cm^{-1})							
	Ab initio[a]	Measured[d]	S (296 K) [c] (10^{-28} cm per molecule)	δ_0	γ_0	ν_{VC}	γ_2	δ_2
Q4	7971.10017(5)	7971.1003352(893)	0.10534(7)	−2.43(14)	4.98	22.38	7.01	0.77
		7971.1003172(893)		−2.95(14)	3.12	35.54		
Q3	8017.18316(5)	8017.1832459(238)	2.3759(6)	−2.93(24)	5.85	21.34	7.23	0.68
		8017.1832460(238)		−3.45(24)	3.87	34.89		
Q2	8051.98773(5)	8051.9878189(114)	3.2982(4)	−3.10(13)	5.80	21.25	7.07	0.62
		8051.9878190(114)		−3.58(13)	3.45	33.26		
Q1	8075.30747(5)	8075.3075806(23)	26.021(3)	−3.25(2)	5.18	20.85	7.18	0.61
		8075.3075803(23)		−3.72(2)	3.21	34.25		
Q1[b]		8075.3075800(10)	25.915(1)	−3.05(4)	6.66	12.24	9.04	1.59
		8075.3075800(10)		−4.25(4)	2.94	25.27		
S0	8406.36086(5)	8406.3609461(20)	15.554(1)	−3.08(1)	4.90	21.72	6.74	0.75
		8406.3609464(20)		−3.64(1)	3.24	34.51		
S1	8604.21519(5)	8604.2152734(10)	52.380(3)	−2.53(3)	6.16	10.77	12.04	1.44
		8604.2152736(10)		−3.75(3)	2.82	26.01		

[a] *Ab initio* values provided by the H2spectre software.[35] [b] Parameters obtained from the separate series of recordings between 2 and 10 Torr (see Table 1 and Experiment section). [c] The given intensity values include the H_2 isotopic abundance factor (0.9997). [d] The listed values have been corrected from the recoil shift on the order of 2.2×10^{-6} cm^{-1} (65 kHz).

leading to much uncertainty on the apparent line position. For this reason, we chose to use the line shape parameters from the constrained fits in the rest of the analysis.

In the second step, all spectra were fitted separately, fixing the line shape parameters to the values determined in the first step, and floating only the position and intensity. Fig. 4

presents the apparent line positions as a function of pressure, for lines Q1 and S0. The zero-pressure line position and the pressure shift coefficient were obtained from a linear regression of the apparent line centers *vs.* pressure. As a clear departure from the linearity is observed at high pressure (see Fig. 4), the linear regression was performed only below 210 Torr. In the case of the Q1 line, we have included an inset corresponding to the separate series of recordings between 2 and 10 Torr. An excellent agreement (better than 20 kHz) was achieved between the two independent determinations of zero-pressure Q1 line positions.

In order to evaluate the impact of the choice of the profile on the zero-pressure positions, we also applied the procedure described above using simpler line profiles: NGP, which does not include the speed dependence of the broadening and shift (γ_2 = 0 and δ_2 = 0), and qSDNGP with δ_2 fixed to zero. The positions obtained with these two simpler profiles are very close but differ importantly from the qSDNGP positions (see Fig. 4). This observation evidences the importance of the speed-dependence of the collisional shift (δ_2) on the apparent line position at a given pressure value. This is reflected by the larger residuals obtained with δ_2 = 0 (Fig. 3a). Nevertheless, as illustrated in Fig. 4, the zero-pressure position is found mostly identical for the different profiles (within a few kHz). The position and line shift values obtained using an NGP profile are included in Table 2. Let us mention that the NGP pressure shift parameters of the Q1–Q4 lines agree with the values retrieved in ref. 17 using a Galatry profile (both NGP and Galatry profiles neglect speed-dependent effects).

From Table 2, it appears that all the values of the profile parameters of the different lines are consistent except those relative to the separate series of Q1 recordings with a maximum pressure of 10 Torr and those of the S1 recordings with a maximum pressure of 45 Torr. This observation indicates that the line parameters depend not only on the chosen profile but also on the maximum pressure of the recordings used for their determination. The reader is referred to ref. 25 and ref. 26 for a detailed discussion of the correlation between the profile parameters and an improved treatment of the Q1 (2-0) and Q1 (3-0) profiles using a corrected Hartmann–Tran profile adjusted to a particular model of the velocity-changing collisions.

Line intensities were floated for each spectrum and obtained as the average of the line intensity values weighted by their fit uncertainty. The agreement between the reported intensities (Table 2) and HITRAN values (Table 1) is excellent: the four determinations of the Q1, S0, and S1 line intensities lead to an average intensity ratio of 1.0013 with a standard deviation less than 0.0020. The largest relative deviation for the very weak Q4 line with an intensity of 1.04×10^{-29} cm per molecule is less than 1%. This level of agreement validates with an unprecedented accuracy the *ab initio* intensity values of ref. 37 reproduced in the HITRAN database.[21] We note that the uncertainty of 10% attached to the HITRAN intensity value is largely overestimated.

Comparison with *ab initio* calculations

In recent years, significant progress has been achieved in the *ab initio* calculations of H_2, HD, and D_2 energy levels.[1–3,36] In these works, the authors performed 4-particle fully variational calculations including relativistic and quantum electrodynamics (QED) effects in the nonadiabatic treatment of the nuclear motion. The resulting calculated transition frequencies of the six H_2 transitions presently studied, as provided by the H2spectre software[35] are included in Table 2. The corresponding deviations from the experimental values are displayed on the lower panel of Fig. 5.

The first observation is that the deviations obtained for Q3, Q2, S0, and S1 are very close, with an average value of 2.51 MHz and a standard deviation of only 63 kHz. The determined Q1

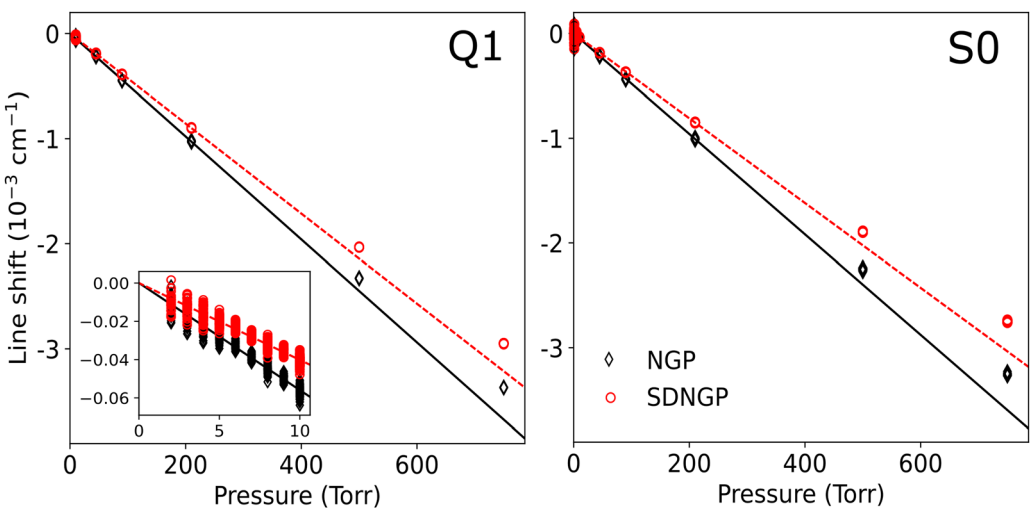

Fig. 4 Determination of the zero-pressure position from a linear extrapolation of the apparent qSDNGP and NGP line positions, for the lines Q1 and S0. The linear regression was performed below 210 Torr due to the clear non-linearity of the observed shift at higher pressures. This plot also illustrates the difference in apparent position due to the inclusion of the speed-dependence of the pressure shift (δ_2), which takes into account the asymmetry of the line profile (see the residuals in Fig. 3). The insert on the Q1 panel corresponds to the separate series of recordings between 2 and 10 Torr (see Text).

transition frequency shows a higher deviation of 3.16 MHz and appears to be an outlier. For comparison purposes, we present on the upper panel of Fig. 5, a similar plot for the six (electric dipole) transitions of HD in the (2-0) band whose transition frequencies were recently measured at high accuracy. The experimental values obtained in the saturation regime[8,10,11] and in the Doppler regime[16,17] have a similar accuracy of a few tens of kHz. Very similar (meas.-calc.) frequency differences are obtained for the six HD transitions, which are on average 1.91 MHz larger than predicted by theory with a standard deviation of only 49 kHz. Let us note that for both H_2 and HD, the calculated frequencies are underestimated and deviate on average by about 1.7 times their claimed uncertainties (1.6 and 1.1 MHz, respectively). The absence of rotational dependence of the deviations leads to the conclusion that the $V = 2$ vibrational term is underestimated by theory, both for H_2 and HD.

While the uncertainties on the *ab initio* transition frequencies are much larger than the corresponding experimental error bars (about one MHz compared to a few tens of kHz), the energy separations between the ground state rotational levels are predicted with much better accuracy, allowing for more stringent validation tests. The lower uncertainty on the energy separation is probably related to error cancellations in the computation of the energy levels.

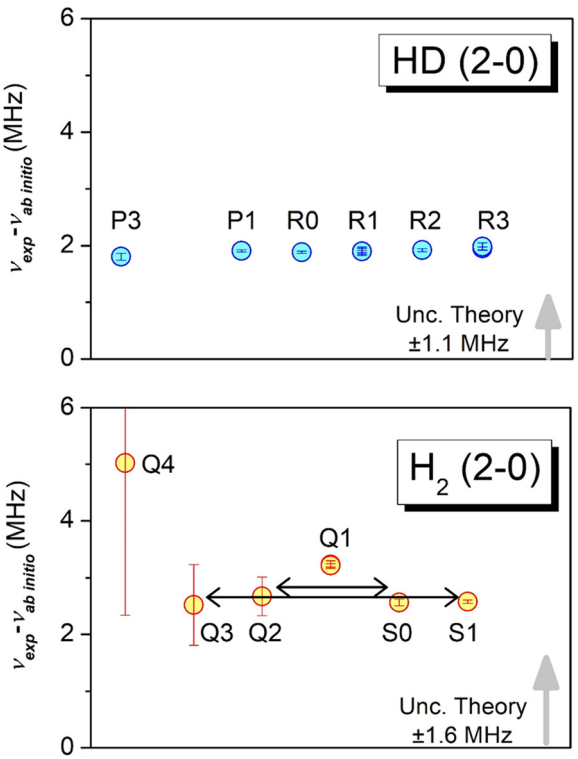

Fig. 5 Differences between experiment and theory for the most accurate experimental frequency determinations in the first overtone band of HD and H_2 (upper and lower panel, respectively). The theoretical values were obtained from the H2spectre software.[35] The grey arrows represent the uncertainty on the calculated values (1.1 and 1.6 MHz, respectively). The H_2 experimental values are obtained in the present work, while the HD experimental values were reported in ref. 8,10,11,16,17. The black arrows on the lower panel connect pairs of transitions involved in ground-state combination relations.

Combination differences in measured transition frequencies can be used to derive accurate values of the energy-level separation in the ground vibrational state. From the six presently measured H_2 (2-0) transition frequencies, the energy separation between the $J = 2$ and $J = 0$ levels, $\Delta_{(J=2)-(J=0)}$ was obtained by difference of S0 and Q2 transition frequencies sharing the same $J = 2$ ($V = 2$) upper level. Similarly, the separation between $J = 3$ and $J = 1$ levels, $\Delta_{(J=3)-(J=1)}$ was obtained by difference of S1 and Q3 transition frequencies. The comparison summarized in Table 3 shows a convincing agreement between theory and experiment, within 100 kHz for both $\Delta_{(J=2)-(J=0)}$ and $\Delta_{(J=3)-(J=1)}$. This level of agreement is surprisingly good as it is better than the uncertainties on the *ab initio* values (110 and 180 kHz, respectively) which are themselves significantly better than the uncertainties on the experimental values (390 and 750 kHz, respectively).

In summary, the experimental data at disposal confirm the sub-MHz accuracy of the energy separation of the *ab initio* ground state energy levels and seem to indicate that the 1.6 MHz claimed uncertainty on the *ab initio* frequencies of the studied (2-0) transitions is underestimated.

Compared to the average value for the Q3, Q2, S0, and S1 positions, the 650 kHz offset of the Q1 frequency difference to theory remains to be explained. We considered a possible experimental bias due to an underlying impurity line located in the range of the Q1 line profile but the typical concentration of water vapor in our spectra leads to a negligible contribution of this species. A systematic search of the possible absorbers on the basis of the HITRAN database indicates that a weak ammonia line could be present in the range of the Q1 profile but the spectra do not show stronger ammonia lines located in the vicinity. Let us recall, that the Q1 transition frequency reported in this work was retrieved from spectra recorded in two measurement campaigns, three years apart and an agreement within 18 kHz is obtained between the two determinations. Thus, the origin of the 650 kHz offset of the Q1 frequency is unexplained so far. As the O3 (2-0) transition at 7488.27 cm^{-1} is sharing the same $J = 1$ ($V = 2$) upper level as the Q1 transition, the (planned) accurate measurement of the O3 transition frequency should bring a decisive confirmation of the existence and the amplitude of this offset.

In summary, the transition frequencies reported in the present work are the most accurate reported so far for H_2, the first ones in the (2-0) band referenced to an absolute frequency standard. Their relative uncertainty is at the 10^{-10} level in the case of the Q1, S0, and S1 transitions. The comparison to the most recent theoretical values shows a systematic underestimation of 2.51 MHz of the calculated transition frequencies, a situation similar to that found for (2-0) transitions in HD. This observation provides a challenge for future refinement of the *ab initio* calculations of the energy levels of the hydrogen molecule. Finally, we note that *ab initio* values of the intensity of the six studied transitions are experimentally validated within a few thousandths.

Table 3 Energy separations between ground state rotational levels obtained by the combination of differences of the measured and calculated transitions. The difference between the $J = 2$ and $J = 0$ energy levels was obtained from the S0 and Q2 transition frequencies, and that between the $J = 3$ and $J = 1$ energy levels was obtained from the S1 and Q3 transition frequencies. The (1σ) uncertainties are given within parenthesis in the unit of the last quoted digit

	Exp. (MHz)	Calc. (MHz)	Exp. (cm^{-1})	Calc. (cm^{-1})
$\Delta_{(J=2)-(J=0)}$	10 623 839.09(39)	10 623 839.17(11)	354.373 127(13)	354.373 130(4)
$\Delta_{(J=3)-(J=1)}$	17 598 777.46(75)	17 598 777.37(18)	587.032 028(25)	587.032 025(6)

Conflicts of interest

There are no conflicts to declare.

Acknowledgements

AOK acknowledges the support of the French National Research Agency in the framework of the ''Investissements d'avenir'' program (ANR-15-IDEX-02). The support by the REFIMEVE consortium (Equipex REFIMEVE+ANR-11-EQPX-0039) and by CNRS (France) in the frame of the International Research Project SAMIA are acknowledged. AOK acknowledges partial support from the Russian State Project No. 0030-2021-0016. Communications with K. Pachucki (Warsaw), J. Komasa (Poznan), W. Ubachs (Amsterdam), and ML. Diouf (Amsterdam) about the *ab initio* values of the H_2 transition frequencies are acknowledged.

References

1 P. Czachorowski, M. Puchalski, J. Komasa and K. Pachucki, *Phys. Rev. A*, 2018, **98**, 052506.
2 M. Puchalski, A. Spyszkiewicz, J. Komasa and K. Pachucki, *Phys. Rev. Lett.*, 2018, **121**, 073001.
3 M. Puchalski, J. Komasa, A. Spyszkiewicz and K. Pachucki, *Phys. Rev. A*, 2019, **100**, 020503.
4 H. Jóźwiak, H. Cybulski and P. Wcisło, *J. Quant. Spectrosc. Radiat. Transfer*, 2020, **256**, 107255.
5 M. Puchalski, J. Komasa and K. Pachucki, *Phys. Rev. Lett.*, 2020, **125**, 253001.
6 P. Dupré, *Phys. Rev. A*, 2020, **101**, 022504.
7 A. Campargue, S. Kassi, K. Pachucki and J. Komasa, *Phys. Chem. Chem. Phys.*, 2012, **14**, 802.
8 F. M. J. Cozijn, P. Dupré, E. J. Salumbides, K. S. E. Eikema and W. Ubachs, *Phys. Rev. Lett.*, 2018, **120**, 153002.
9 F. M. J. Cozijn, M. L. Diouf, V. Hermann, E. J. Salumbides, M. Schlösser and W. Ubachs, *Phys. Rev. A*, 2022, **105**, 062823.
10 M. L. Diouf, F. M. J. Cozijn, B. Darquié, E. J. Salumbides and W. Ubachs, *Opt. Lett.*, 2019, **44**, 4733.
11 M. L. Diouf, F. M. J. Cozijn, K.-F. Lai, E. J. Salumbides and W. Ubachs, *Phys. Rev. Res.*, 2020, **2**, 023209.
12 T.-P. Hua, Y. R. Sun and S.-M. Hu, *Opt. Lett.*, 2020, **45**, 4863.
13 A. Fast and S. A. Meek, *Phys. Rev. Lett.*, 2020, **125**, 023001.
14 M. L. Niu, E. J. Salumbides, G. D. Dickenson, K. S. E. Eikema and W. Ubachs, *J. Mol. Spectrosc.*, 2014, **300**, 44.
15 A. Castrillo, E. Fasci and L. Gianfrani, *Phys. Rev. A*, 2021, **103**, 022828.
16 A. Castrillo, E. Fasci and L. Gianfrani, *Phys. Rev. A*, 2021, **103**, 069902.
17 S. Kassi, C. Lauzin, J. Chaillot and A. Campargue, *Phys. Chem. Chem. Phys.*, 2022, **24**, 23164.
18 C.-F. Cheng, Y. R. Sun, H. Pan, J. Wang, A. W. Liu, A. Campargue and S.-M. Hu, *Phys. Rev. A: At., Mol., Opt. Phys.*, 2012, **85**, 024501.
19 S.-M. Hu, H. Pan, C.-F. Cheng, X.-F. Li, J. Wang, A. Campargue and A. W. Liu, *Astrophys. J.*, 2012, **749**(1), 76.
20 S. Kassi and A. Campargue, *J. Mol. Spectrosc.*, 2014, **300**, 55.
21 I. E. Gordon, L. S. Rothman, R. J. Hargreaves, R. Hashemi and E. V. Karlovets, *et al.*, *J. Quant. Spectrosc. Radiat. Transf.*, 2021, **277**, 107949.
22 S. L. Bragg, J. W. Brault and W. H. Smith, *Astrophys. J.*, 1982, **263**, 999.
23 P. Wcislo, H. Tran, S. Kassi, A. Campargue, F. Thibault and R. Ciurylo, *J. Chem. Phys.*, 2014, **141**, 074301.
24 P. Wcisło, I. E. Gordon, H. Tran, Y. Tan, S.-M. Hu, A. Campargue, S. Kassi, D. Romanini, C. Hill, R. V. Kochanov and L. S. Rothman, *J. Quant. Spectrosc. Radiat. Transfer*, 2016, **177**, 75.
25 D. Mondelain, T. Sala, S. Kassi, D. Romanini, M. Marangoni and A. Campargue, *J. Quant. Spectrosc. Radiat. Transfer*, 2015, **154**, 35.
26 D. Mondelain, S. Kassi, T. Sala, D. Romanini, M. Marangoni and A. Campargue, *J. Mol. Spectrosc.*, 2016, **326**, 5.
27 M. Konefał, S. Kassi, D. Mondelain and A. Campargue, *J. Quant. Spectrosc. Radiat. Transfer*, 2020, **241**, 106653.
28 S. Vasilchenko, H. Tran, D. Mondelain, S. Kassi and A. Campargue, *J. Quant. Spectrosc. Radiat. Transfer*, 2019, **235**, 332.
29 B. Bordet, S. Kassi and A. Campargue, *J. Quant. Spectrosc. Radiat. Transfer*, 2021, **260**, 107453.
30 D. Mondelain, S. Vasilchenko, S. Kassi and A. Campargue, *J. Quant. Spectrosc. Radiat. Transfer*, 2020, **253**, 107020.
31 W. Meyer, A. Borysow and L. Frommhold, *Phys. Rev. A: At., Mol., Opt. Phys.*, 1993, **47**, 4065.
32 M. Abel, L. Frommhold, X. Li and K. L. C. Hunt, *J. Phys. Chem. A*, 2011, **115**(25), 6805.
33 E. M. Adkins, MATS: Multi-spectrum Analysis Tool for Spectroscopy, 2020.
34 A. O. Koroleva, S. N. Mikhailenko, S. Kassi and A. Campargue, *J. Quant. Spectrosc. Radiat. Transfer*, 2023, **298**, 108489.
35 P. Czachorowski, H2SPECTRE version 7.3, Fortran source code, 2020, PhD thesis, University of Warsaw, 2019, **https://www.fuw.edu.pl/~krp/codes.html**; **http://qcg.home.amu.edu.pl/H2Spectre.html**.
36 J. Komasa, K. Piszczatowski, G. Łach, M. Przybytek, B. Jeziorski and K. Pachucki, *J. Chem. Theory Comput.*, 2011, **7**(10), 3105.
37 L. Wolniewicz, I. Simbotin and A. Dalgarno, *Astrophys. J., Suppl. Ser.*, 1998, **115**, 293.

